



## The QCD vacuum

Pierre van Baal <sup>a</sup>

<sup>a</sup>Instituut-Lorentz for Theoretical Physics, University of Leiden,  
PO Box 9506, NL-2300 RA Leiden, The Netherlands

We review issues involved in understanding the vacuum, long-distance and low-energy structure of non-Abelian gauge theories and QCD. The emphasis will be on the role played by instantons.

### 1. INTRODUCTION

The term “QCD vacuum” is frequently abused. Only in the case of the Hamiltonian formulation is it clear what we mean by the vacuum: it is the wave functional associated with the lowest energy state. Observables create excitations on top of this vacuum. Knowing the vacuum is knowing all: We should know better.

Strictly speaking the vacuum is empty. Nevertheless its wave functional can be highly non-trivial, deviating considerably from that of a non-interacting Fock space, based on a quadratic theory. Even in the later case the result of probing the vacuum by boundaries is non-trivial as we know from Casimir. The probe is essential: one needs to disturb the vacuum to study its properties. Somewhat perversely the vacuum may be seen as a relativistic aether. It promises to magically resolve our problems, from confinement to the cosmological constant. For the latter supersymmetry is often called for to remove the otherwise required fine-tuning. It merely hides the relativistic aether, even giving it further structure. Remarkably it seems to have enough structure to give a non-trivial example of the dual superconductor at work [1].

Most will indeed put their bet on the dual superconductor picture for the QCD vacuum [2], and this has motivated the hunt for magnetic monopoles using lattice techniques, long before supersymmetric duality stole the show [1]. The definitions rely on choosing an abelian projection [3] and the evidence is based on the notion of abelian dominance [4], establishing the dual Meissner effect [5], or the construction of

a magnetically charged order parameter, whose non-zero expectation value implies spontaneous breaking of the dual gauge symmetry [6], yielding electric confinement. But center vortices, probed by the newly defined center dominance, this year suddenly became center stage [7] again and we will surely hear more next year.

In the euclidean path integral only the vacuum state will contribute when we let the (imaginary) time go to infinity, underlying the essence of the transfer matrix approach to extract observables from euclidean path integrals as used in lattice gauge theories. However, this is not what people have in mind when talking about the vacuum structure of gauge theories. More appropriate for most studies would be to talk about the low-energy and long-distance behaviour of the theory. One way to address this is to attempt to isolate the relevant degrees of freedom for which one can derive an effective low-energy theory. Monopole actions derived from block-spin transformations [8] and the instanton liquid model [9] are examples. It is not required that the relevant degrees of freedom are associated to semi-classical objects, the main reason being that in a strongly interacting theory the quantum fluctuations can be (much) bigger than the classical effects. Sometimes this argument is used against the relevance of instantons, which by their very definition as localised objects in time might lose significance when quantum fluctuations are too strong.

Due to the limited space available this review concentrates on the instanton content of the theory, where recently considerable progress has been achieved. But first I will use this opportunity to explain my own thoughts on the matter.

## 2. VACUUM DEMOCRACY

The model we wish to describe here starts from the physics in a small volume, where asymptotic freedom guarantees that perturbative results are valid. The assumption is made, that at least for low-energy observables, integrating out the high-energy degrees of freedom is well-defined perturbatively and all the non-perturbative dynamics is due to a few low-lying modes. This is most easily defined in a Hamiltonian setting, since we are interested in situations where the non-perturbative effects are no longer described by semiclassical methods.

### 2.1. Complete gauge fixing

Due to the action of the gauge group on the vector fields, a finite dimensional slice through the physical configuration space (gauge inequivalent fields) is bounded. One way to demonstrate this is by using the complete Coulomb gauge fixing, achieved by minimising the  $L^2$  norm of the gauge field along the gauge orbit. At small energies, fields are sufficiently smooth for this to be well defined and it can be shown that the space under consideration has a boundary, defined by points where the norm is degenerate. These are by definition gauge equivalent such that the wave functionals are equal, possibly up to a phase factor in case the gauge transformation is homotopically non-trivial. The space thus obtained is called a fundamental domain. For a review see ref. [10].

### 2.2. Non-perturbative dynamics

Given a particular compact three dimensional manifold  $M$  on which the gauge theory is defined, scaling with a factor  $L$  allows one to go to larger volumes. It is most convenient to formulate the Hamiltonian in scale invariant fields  $\hat{A} = LA$ . Dividing energies by  $L$  recovers the  $L$  dependence in the classical case, but the need of an ultraviolet cutoff and the resulting scale anomaly introduces a running coupling constant  $g(L)$ , which in the low-energy effective theory is the only remnant of the breaking of scale invariance.

When the volume is very small, the effective coupling is very small and the wave functional is highly localised, staying away from the boundaries of the fundamental domain. We may com-

pare with quantum mechanics on the circle, seen as an interval with identifications at its boundary. At which points we choose these boundaries is just a matter of (technical) convenience. The fact that the circle has non-trivial homotopy, allows one to introduce a  $\theta$  parameter (playing the role of a Bloch momentum).

Expressed in  $\hat{A}$ , the shape of the fundamental domain and the nature of the boundary conditions, is independent of  $L$ . Due to the rise of the running coupling constant with increasing  $L$  the wave functional spreads out over the fundamental domain and will start to feel the boundary identifications. This is the origin of non-perturbative dynamics in the low-energy sector of the theory.

Quite remarkably, in all known examples (for the torus and sphere geometries), the sphalerons lie exactly at the boundary of the fundamental domain, with the sphaleron mapped into the anti-sphaleron by a homotopically non-trivial gauge transformation. The sphaleron is the saddle point at the top of the barrier reached along the tunnelling path associated with the largest instanton, its size limited by the finite volume.

For increasing volumes the wave functional first starts to feel the boundary identifications at these sphalerons, “biting its own tail”. When the energy of the state under consideration becomes of the order of the energy of this sphaleron, one can no longer use the semiclassical approximation to describe the transition over the barrier and it is only at this moment that the shift in energy becomes appreciable and causes sizeable deviations from the perturbative result. This is in particular true for the groundstate energy. Excited states feel these boundary identifications at somewhat smaller volumes, but nodes in their wave functional near the sphaleron can reduce or postpone the influence of boundary identifications.

This has been observed clearly for  $SU(2)$  on a sphere [11]. The scalar and tensor glueball mass is reduced considerably due to the boundary identifications, whereas the oddball remains unaffected (see fig. 1). These non-perturbative effects remove an unphysical near-degeneracy in perturbation theory (with the pseudoscalar even slightly lower than the scalar glueball mass). The dominating configurations involved are associated to

instanton fields, in a situation where semiclassical techniques are inappropriate for computing the magnitude of the effect. When boundary identifications matter, the path integral receives large contributions from configurations that have non-zero topological charge, and in whose background the fermions have a chiral zero mode, its consequences to be discussed later.

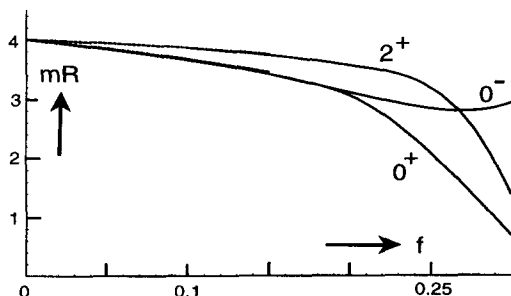


Figure 1. The low-lying glueball spectrum on a sphere of radius  $R$  as a function of  $f = g^2(R)/2\pi^2$  at  $\theta = 0$ . Approximately,  $f = 0.28$  corresponds to a circumference of 1.3 fm. From ref. [11].

At some point technical control is lost, since so far only the appropriate boundary conditions near the sphalerons can be implemented. As soon as the wave functional starts to become appreciable near the rest of the boundary too, this is no longer sufficient.

This method has in particular been very successful to determine the low-lying spectrum on the torus in intermediate volumes, where for  $SU(2)$  agreement with the lattice Monte Carlo results has been achieved within the 2% statistical errors [10,12]. In this case the non-perturbative sector of the theory was dominated by the energy of electric flux (torolon mass), which vanishes to all orders in perturbation theory. The leading semiclassical result is  $\exp(-S_0/g(L))$ , due to tunnelling through a quantum induced barrier of height  $E_s = 3.21/L$  and action  $S_0 = 12.5$ . Already beyond 0.1 fm this approximation breaks down. One finds, accidentally in these small volumes, the energy to be nearly linear in  $L$ .

The effective Hamiltonian in the zero-momentum gauge fields, derived by Lüscher [13], and later augmented by boundary identifications to include the non-perturbative effects [12], breaks

down at the point where boundary identifications in the non-zero momentum directions associated with instantons become relevant. The sphaleron has an energy  $72.605/(Lg^2(L))$  and was constructed numerically [14]. Its effect becomes noticeable beyond volumes of approximately  $(0.75 \text{ fm})^3$ . For  $SU(3)$  this was verified directly in a lattice Monte Carlo calculation of the finite volume topological susceptibility [15]. The results for the sphere have shown that also these effects can in principle be included reliably, but the lack of an analytic instanton solution on  $T^3 \times \mathbb{R}$  has prevented us from doing so in practise.

### 2.3. Domain formation

The shape of the fundamental domain depends on the geometry. Assuming that  $g(L)$  keeps on growing with increasing  $L$ , causing the wave functional to feel more and more of the boundary, one would naturally predict that the infinite volume limit depends on the geometry. This is clearly unacceptable, but can be avoided if the ground state obtained by adiabatically increasing  $L$  is not stable. Thus we conjecture that the vacuum is unstable against domain formation. This is the minimal scenario to make sure that at large volumes, the spectrum is independent of its geometry. Domains would naturally explain why a non-perturbative physical length scale is generated in QCD, beyond which the coupling constant will stop running. However, we have no guess for the order parameter, let alone an effective theory describing excitations at distances beyond these domains. Postulating their existence, nevertheless a number of interesting conclusions can be drawn.

The best geometry to study domain formation is that of a box since it is space-filling. We can exactly fill a larger box by smaller ones. This is not true for most other geometries. In small to intermediate volumes the vacuum energy density is a decreasing function [12] of  $L$ , but in analogy to the double well problem one may expect that at stronger coupling the vacuum energy density rises again with a minimum at some value  $L_0$ , assumed to be 0.75 fm. For  $L$  sufficiently larger than  $L_0$  it thus becomes energetically favourable to split the volume in domains of size  $L_0^3$ .

Since the ratio of the string tension to the

scalar glueball mass squared shows no structure around  $(0.75 \text{ fm})^3$ , we may assume that both have reached their large volume value within a domain. The nature of their finite size corrections is sufficiently different to expect these not to cancel accidentally. The colour electric string arises from the fact that flux that enters the box has to leave it in the opposite direction. Flux conservation with these building blocks automatically leads to a string picture, with a string tension as computed within a single domain and a transverse size of the string equal to the average size of a domain,  $0.75 \text{ fm}$ . The tensor glueball in an intermediate volume is heavily split between the doublet ( $E^+$ ) and triplet ( $T_2^+$ ) representations of the cubic group, with resp. 0.9 and 1.7 times the scalar glueball mass. This implies that the tensor glueball is at least as large as the average size of a domain. Rotational invariance in a domain-like vacuum comes about by averaging over all orientations of the domains. This is expected to lead to a mass which is the multiplicity weighted average of the doublet and triplet, yielding a mass of 1.4 times the scalar glueball mass. Domain formation in this picture is *driven* by the large field dynamics associated with sphalerons. Which state gets affected most depends in an intricate way on the behaviour of the wave functionals (cmp. fig. 1).

In the four dimensional euclidean context,  $O(4)$  invariance makes us assume that domain formation extends in all four directions. As is implied by averaging over orientations, domains will not neatly stack. There will be dislocations which most naturally are gauge dislocations. A point-like gauge dislocation in four dimensions is an instanton, lines give rise to monopoles and surfaces to vortices. In the latter two cases most naturally of the  $Z_N$  type. We estimate the density of these objects to be one per average domain size. We thus predict an instanton density of  $3.2 \text{ fm}^{-4}$ , with an average size of  $1/3 \text{ fm}$ . For monopoles we predict a density of  $2.4 \text{ fm}^{-3}$ .

If an effective colour scalar field will play the role of a Higgs field, abelian projected monopoles will appear. It can be shown [16] that a monopole (or rather dyon) loop, with its  $U(1)$  phase rotating  $Q$  times along the loop (generating an electric field), gives rise to a topological charge  $Q$ .

In abelian projection it has been found that an instanton always contains a dyon loop [17]. We thus argue this result to be more general, leading to further ties between monopoles and instantons.

## 2.4. Regularisation and $\theta$

It is useful to point out that the non-trivial homotopy of the physical configuration space, like non-contractable loops associated to the instantons ( $\pi_1(\mathcal{A}/\mathcal{G}) = \pi_3(G) = \mathbb{Z}$ ), is typically destroyed by the regularisation of the theory. This is best illustrated by the example of quantum mechanics on the circle. Suppose we replace it by an annulus. As long as the annulus does not fill the hole, or we force the wave function to vanish in the middle,  $\theta$  is a well-defined parameter associated to a multivalued wave function. We may imagine the behaviour for small instantons in gauge theories to be similar to that at the center in the above model. Indeed, the gauge invariant geodesic length of the tunnelling path for instantons on  $M \times \mathbb{R}$ , given by  $\ell = \int_{-\infty}^{\infty} dt \sqrt{\mathcal{V}(t)}$ , where  $\mathcal{V}(t)$  is the classical potential along the tunnelling path, is expected to vanish for instantons that shrink to zero size. This is confirmed for  $M = S^3$ , using results of ref. [18] to show that (for unit radius)  $\ell = 2\Gamma^2(\frac{3}{4})\sqrt{6\pi/b}(1 + \mathcal{O}(b^{-\frac{3}{2}}))$ , with the instanton size defined by  $\rho \equiv (1+b^2)^{-\frac{1}{2}}$ .

Due to the need of regularising the ultraviolet behaviour, the small instantons are cut out of the theory. Using the lattice regularisation this does not leave a hole, but rather removes the “singularity at the origin”, as the lattice configuration space has no non-contractable loops. Strictly speaking this means one can not have a  $\theta$  parameter at any finite lattice spacing. Furthermore the regularisation forces one to divide out all the gauge transformations as there are no homotopically non-trivial ones. It is advisable to divide out *all* gauge transformations, even if some of the homotopy is preserved by some regularisation!

One can, however, still introduce the  $\theta$  parameter by adding  $i\theta Q$  (with  $Q = \int d_4x q(x)$ ,  $q(x) = \text{Tr}(F^{\mu\nu}(x)\tilde{F}_{\mu\nu}(x))/16\pi^2$  the topological charge operator) to the action. Of course only for smooth fields the charge  $Q$  will be (approximately) integer. Also within the Hamiltonian formulation one may introduce a  $\theta$  parameter

ter by mixing the electric field with  $\theta$  times the magnetic field,  $E \rightarrow E - \theta B/(2\pi)^2$ . In these approaches  $\theta$  is simply a parameter added to the theory. Whether or not one will retrieve the expected periodic behaviour in the continuum limit becomes a dynamical question.

It should be pointed out that in particular for  $SU(N)$  gauge theories in a box (in sectors with non-trivial magnetic flux) there is room to argue for a  $2\pi N$ , as opposed to a  $2\pi$ , periodicity for the  $\theta$  dependence. However, the spectrum is periodic with a period  $2\pi$ , and the apparent discrepancy is resolved by observing that there is a non-trivial spectral flow [19]. This may lead to phase transitions at some value(s) of  $\theta$ , related to the oblique confinement mechanism [3]. Similarly for supersymmetric gauge theories this interpretation, supported by the recent discovery of domain walls between different vacua [20], removes the need for semiclassical objects with a charge  $1/N$ . Such solutions do exist for the torus, but the fractional charge is related to magnetic flux and the interpretation is necessarily as stated above! The “wrong” periodicity in  $\theta$  has long been used to argue against the relevance of instantons, but in the more recent literature this is now phrased more cautiously [21,22].

### 3. INSTANTONS

Instantons are euclidean solutions responsible for the axial anomaly, breaking the  $U_A(1)$  subgroup of the  $U(N_f) \times U(N_f)$  chiral symmetry for  $N_f$  flavours of massless fermions [23], as dictated by the anomaly,  $\sum_f \partial_\mu \bar{\Psi}_f \gamma^\mu \gamma_5 \Psi_f(x) = 2N_f q(x)$ . The breaking of  $U_A(1)$  manifests itself in the semiclassical computations through the presence of fermion zero modes, with their number and chirality fixed by the topological charge, through the Atiyah-Singer index theorem [24]. Integration over the fermion zero modes leads to the so-called ’t Hooft vertex or effective interaction [23]. The integration over the scale parameter of the instanton ensemble is infrared dominated and a non-perturbative computation is desirable.

In addition it is believed that the instantons are responsible for chiral symmetry breaking, where a chiral condensate is formed, which breaks the

axial gauge group  $U_A(N_f)$  completely. This spontaneous breaking is dynamical and it is less well established that instantons are fully responsible. It is the basis of the instanton liquid model as developed by Shuryak over the years. For a comprehensive recent review see ref. [9]. The details of the instanton ensemble play an important role. Only a liquid-like phase, as opposed to the dilute or crystalline phases, will give rise to a chiral condensate. The model also makes a prediction for the average size and the topological susceptibility. In particular the latter quantity should be well-defined beyond a semiclassical approximation. For large sizes the instanton distribution is exponentially cut-off and instantons do not give rise to an area law for the Wilson loop. When large instantons are more weakly suppressed the situation may differ [25], but a semiclassical analysis in this case should not be trusted.

Remarkably the topological susceptibility in pure gauge theories can be related to the  $\eta'$  mass through the so-called Witten-Veneziano relation,  $f_\pi^2(m_\eta^2 + m_\eta'^2 - 2m_K^2)/2N_f = \int d_4x \langle T(q(x)q(0)) \rangle_R \equiv \chi_t$ , leading to the prediction  $\chi_t \sim (180 \text{ MeV})^4$ . This is based on the fact that the  $U_A(1)$  symmetry is restored in the planar limit [26,27], with  $\chi_t$  of order  $1/N^2$ . From the requirement that in the presence of massless quarks  $\chi_t$  (and the  $\theta$  dependence) disappears, the pure gauge susceptibility can be related to the quark-loop contributions in the pseudoscalar channel. Pole dominance requires the lightest pseudoscalar meson to have a mass squared of order  $1/N$ . Relating the residue to the pion decay constant gives the desired result [27]. The index  $R$  indicates the necessity of equal-time regularisation [26]. A derivation on the lattice using Wilson and staggered fermions was obtained in ref. [28], making use of Ward-Takahashi identities. Finally, also the coarse grained partition function of the instanton liquid model [9] allows one to directly determine the ’t Hooft effective Lagrangian [23], from which the Witten-Veneziano formula can be read off [29]. This formula is almost treated as the holy grail of instanton physics. It is important to realise that some approximations are involved, although it is gratifying there are three independent ways to obtain it [26–29].

### 3.1. Field theoretic method

A direct computation of  $\chi_t = \int d_4x \langle q(x)q(0) \rangle$  on the lattice requires a choice of discretisation for the charge density. A particularly simple one is [30]  $q_L(x) = -\sum \text{Tr}(U_{\mu\nu}(x)\tilde{U}_{\mu\nu}(x))/16\pi^2$ , where  $\tilde{U}_{\mu\nu}(x) = \frac{1}{2}\varepsilon_{\mu\nu\rho\sigma}\tilde{U}_{\rho\sigma}(x)$  is the clover averaged plaquette  $P_{\mu\nu}(x)$ , formed by the four plaquettes that meet at  $x$ . Due to the short distance singularities the operators require renormalisations. The lattice charge operator is conjectured to satisfy  $Q_L = \sum_x q_L(x) = a^4 Q Z(\beta) + \mathcal{O}(a^6)$ , correcting for the fact that  $Q_L$  need not be integer. In addition an additive renormalisation, associated to the contact term discussed before [26], arises due to mixing of  $\chi_L$  with operators with the same quantum numbers,  $\chi_L = a^4 \chi_t Z^2(\beta) + M(\beta) + \mathcal{O}(a^6)$ .

To determine  $Z(\beta)$  and  $M(\beta)$  one takes a classical configuration with a fixed topological charge  $Q$  [31]. Monte Carlo updates are rejected if they change the charge as determined by cooling and subsequent measurements of  $Q_L$  and  $\chi_L$  allows one to extract  $Z$  and  $M$ . (In a sector with fixed charge  $Q$  we note that  $\chi_t = Q^2/V$ , with  $V$  the volume.) Over a certain range, independence of the starting configuration and the volume has been observed and was henceforth assumed [31]. Due to the need to fix  $Q$  to determine the renormalisation factors, this is in a sense a hybrid method, and might also be sensitive to some of the problems of cooling - to be discussed shortly.

Considerable progress has been achieved, however, by repeating the study with other choices for  $q_L$ , based on smearing the links (iteratively replacing them by staples). This considerably reduces the value of  $M$ , greatly facilitating the extraction of a signal. On a  $16^4$  lattice one finds  $\chi_t = (175(5) \text{ MeV})^4$  (for  $SU(3)$  at  $\beta = 5.9, 6.0$  and  $6.1$ ) and  $\chi_t = (198(8) \text{ MeV})^4$  (for  $SU(2)$  at  $\beta = 2.44, 2.5115$  and  $2.57$ ). For the discussion on finite temperature, how the scale was set and for further details and references see ref. [31].

### 3.2. Cooling

In the continuum, the Schwartz inequality implies that the action of any field configuration with charge  $Q$  is bounded by  $8\pi^2|Q|$ , and is reached by (anti-)selfdual solutions. In its simplest form, cooling aims at finding this min-

imal action, using it to identify the topological charge. As all quantum fluctuations are removed, no renormalisations are required, such that  $\chi_t = \langle Q^2 \rangle / V$ , where the average is over the Monte Carlo ensemble. Cooling can be achieved by putting  $\beta = \infty$  in the standard Monte Carlo update (accepting updates only if they lower the action). The same result is obtained by a sort of congruent gradient method, which uses the lattice equations of motion to lower the action [32]. For  $SU(2)$  this method is deterministic and allows for estimating its rate of convergence [14].

It is a remarkable and deep mathematical property of non-Abelian gauge theories on a compact four dimensional manifold that exact  $SU(N)$  solutions exist for any charge  $Q$  with  $4N|Q|$  parameters (moduli), in general describing position, size and colour orientation of  $|Q|$  pseudoparticles. Although a compact manifold breaks the scale invariance, generically instantons with arbitrary size exist, only limited by the finite volume. A notable exception is charge one instantons on  $T^4$ . There is no problem in having smooth configurations of unit charge, but in an attempt to make them self-dual they shrink to a point [33].

To understand its implications we take the time direction to infinity, in which case finite action forces tunnelling from vacuum to vacuum configuration. The vacuum on a torus is, however, not unique. Periodic boundary conditions in the time direction force the vacua at both ends to be the same and as soon as one releases this constraint, exact vacuum to vacuum tunnelling solutions exist. This was studied for  $O(3)$  through the exact solutions on a cylinder [34]. For gauge theories it can be proven that twisted (for  $SU(2)$  “anti-periodic”) boundary conditions [19] remove the obstruction, even at finite  $T$ . Large instantons have finite size effects [35] of  $\mathcal{O}(1/T)$ . For sufficiently large volumes, assuming the instanton size will be cutoff dynamically, the effect is irrelevant, further helped by the fact that in a large volume almost all configurations have higher charges.

As always, the continuum limit competes with the infinite volume limit. Even with presentday computer power, the remaining window is uncomfortably small. The above finite size effect is usually swamped by the cutoff effects. As the lattice

cutoff breaks the scale and rotational invariance, we would expect that the action is no longer constant on the continuum moduli space. Indeed, for a smooth instanton the Wilson action behaves as  $S_W(\hat{\rho} \equiv \rho/a) = 8\pi^2(1 - \hat{\rho}^{-2}/5 + \mathcal{O}(\hat{\rho}^{-4}))$  and causes the instanton to shrink, until it becomes of the size of the cutoff and falls through the lattice. Cooling will first remove high-frequency modes and one is left with a slow motion along the moduli space, giving rise to a plateau in the cooling history, used to identify the topological charge. One will miss instantons smaller than some fixed value  $\hat{\rho}_c$ . Assuming asymptotic freedom, one easily shows that the error vanishes in the continuum limit. Note that by construction, the cooling method never will associate charge to a dislocation with an action smaller than  $96\pi^2/11N$ , the entropic bound, which would spoil scaling [36].

For extracting the size distribution, cooling and under-relaxed (or slow) cooling [37] is problematic as the size clearly will depend on where along the plateau one analyses the data [38]. The size distribution can be made to scale properly only at the expense of carefully adjusting the number of cooling steps [39] when going to different  $\beta$ .

One can avoid losing instantons under cooling by modifying the action such that the scaling violations change sign [35], for example by adding a  $2 \times 2$  plaquette to the Wilson action. This so-called over-improved action has the property that instantons grow under cooling, until stopped by the finite volume. Consequently it would still mutilate the size distribution. This can be avoided by improving the action so as to minimise the scaling violations [40]. A particularly efficient choice is the so-called five-loop improved (5Li) lattice action:  $S_{5Li} = \sum_{m,n} c_{m,n} \sum_{x,\mu\nu} \text{Tr}(1 - P_{m\mu,n\nu}(x))$ , where  $P_{m\mu,n\nu}(x)$  is the  $m \times n$  plaquette and  $c_{1,1} = \frac{65}{36}$ ,  $c_{2,2} = -\frac{11}{720}$ ,  $c_{1,2} = -\frac{8}{45}$ ,  $c_{1,3} = \frac{1}{90}$  and  $c_{3,3} = \frac{1}{1620}$ . Overimproved cooling [35] is defined by  $c_{1,1} = (4 - \varepsilon)/3$  and  $c_{2,2} = (\varepsilon - 1)/48$ , which is  $\mathcal{O}(a^2)$  improved for  $\varepsilon = 0$ . The 5Li is improved to  $\mathcal{O}(a^4)$  and allows for a tiny action barrier of less than one permill of the instanton action at  $\hat{\rho}_c = 2.3$ . Instantons of smaller size will be rapidly lost under cooling, but larger ones will stay forever and practically not change their size, of course using twisted boundary conditions. For

$\hat{\rho} > 4$  the action is at most a factor  $10^{-4}$  larger than its continuum value. After thus eliminating the cutoff effects, the finite size effects in the charge one sector are clearly observed, see fig. 2.

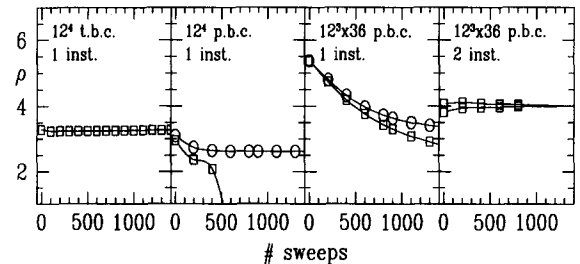


Figure 2. Cooling history [40] for  $SU(2)$  charge one (and two) instanton with twisted and periodic boundary conditions. Squares represent 5Li and circles over-improved cooling ( $\varepsilon = -1$ ).

It is important to note that improved cooling [40] is used as a diagnostic tool; the configurations are still generated by the standard Wilson action. One may of course also use improved actions for this purpose, but the 5Li action was simply not tuned dynamically. One difficulty in extracting the instanton distribution is that a typical ensemble will have both instantons and anti-instantons. These interact, although the action only slightly differs from  $8\pi^2$  times the number of pseudoparticles, provided they are not too close. Close instanton anti-instanton (I-A) pairs will annihilate. Cooling sufficiently long also removes more widely separated pairs. As the cooling makes the configuration smooth, the total charge can be measured reliably even in the presence of these pairs. For  $SU(2)$ , lattices of sizes  $12^4$  and  $12^3 \times 36$  at  $\beta = 2.4$  and  $2.5$  with periodic and twisted boundary conditions, as well as  $24^4$  at  $\beta = 2.6$  with twisted boundary conditions were used. At  $\beta = 2.5$  a physical volume of  $1.02 \text{ fm}$  across gives sizable finite size corrections. One obtains  $\chi_t = (200(15) \text{ MeV})^4$  with good scaling properties [40], which agrees with ref. [31].

Extracting the size of an instanton is based on identifying the pseudoparticles. Using among other things the known profile of an isolated instanton, five different definitions for the size  $\rho$  were used, which are all well correlated [40]. The resulting size distribution is given in fig. 3, com-

binning results for  $\beta=2.4$  (averaged over the different lattice types and boundary conditions after 20 cooling sweeps) and for  $\beta=2.6$  (after 50 cooling sweeps). The solid curve is a fit to the formula  $P(\rho) \propto \rho^{7/3} \exp(-(\rho/w)^p)$ , with  $w = 0.47(9)$  fm and  $p = 3(1)$ , which at small sizes coincides with the semiclassical result [23]. The peak of this distribution occurs at  $\rho = 0.43(5)$  fm. Under prolonged cooling, up to 300 sweeps, I-A instanton annihilations and in particular finite size effects in the charge one sector do affect the distribution somewhat, but not the average size, which therefore seems to be quite a robust result.

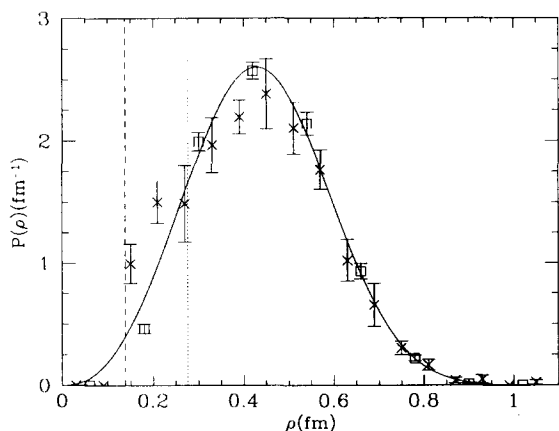


Figure 3.  $SU(2)$  instanton size distribution for  $\beta = 2.4$  (squares) and  $2.6$  (crosses) in a volume  $1.44$  fm across at lattice spacings  $a = 0.12$  and  $0.06$  fm. The dotted and dashed lines represent the cutoff at  $a\rho_c$  for both lattices. From ref. [40].

It would be advantageous if one could come up with a definition for the size that is related to a physical quantity, since now the notion is based on the semiclassical picture. This is nevertheless appropriate for the comparison with the instanton liquid. The relatively large value of the average size as compared to that of  $1/3$  fm predicted by the instanton liquid [9] is a point of worry, typically leading to stronger interactions that may lead to a crystal (without chiral symmetry breaking), rather than a liquid. Nevertheless, in ref. [40] it has been tested that the pseudoparticles are homogeneously distributed with a density of  $2-3$  fm $^{-4}$  and occupying nearly half the volume. This is the case when only close I-A pairs have annihilated and therefore depends on

the amount of improved cooling. It does, however, show that the pseudoparticles are relatively dense (more so than assumed in the instanton liquid [9]). The value of  $3.2$  fm $^{-4}$  for the density, derived earlier in the context of the domain picture is quite realistic in the light of these results.

### 3.3. Smoothing

Another method to study instantons on the lattice is based on the classical fixed point actions [41], defined through the saddle point equation  $S^{FP}(V) = \min_{\{U\}} (S^{FP}(U) + \kappa T(U, V))$ . It is obtained as the weak coupling limit of the blocking transformation with a positive definite kernel  $\kappa T(U, V)$ , which maps a lattice  $\{U\}$  to  $\{V\}$ , coarser by a factor two. Reconstructing the fine from the coarse lattice is called inverse blocking.

It can be shown to map a solution of the lattice equations of motion to a solution on the finer lattice with the same action. Iterating the inverse blocking, the lattice can be made arbitrarily fine, thereby proving the absence of scaling violations to any power in the lattice spacing [41]. This classically perfect action still loses instantons below a critical size, which is typically smaller than a lattice spacing. For solutions this most likely happens at the point where the continuum interpolation of the lattice field is ambiguous, causing the integer geometric charge [42] to jump. For rough configurations that are not solutions, inverse blocking typically reduces the action by a factor 32 and makes it more smooth. The fixed point topological charge is defined as the limiting charge after repeated inverse blockings. This guarantees no charge will be associated to dislocations (of any action below the instanton action).

The classical fixed point action, although optimised to be short range, still has an infinite number of terms and finding a suitable truncation is a practical problem. From examples of parametrisations, the success of reducing scaling violations in quantities like the heavy quark potential (tested by restoring rotational invariance) is evident, for recent reviews see ref. [45]. In practice only a limited number of inverse blockings is feasible and the fixed point topological charge has to rely on a rapid convergence. The closer one is able to construct the fixed point action the bet-



ter this convergence is expected to be. For two dimensional non-linear sigma models sufficient control was achieved to demonstrate that more than one inverse blocking did not appreciably change the topological charge [43].

In four dimensional gauge theories, both finding a manageable parametrisation and doing repeated inverse blockings is a major effort. It goes without saying that if no good approximation to the fixed point action is used, one cannot rely on its powerful theoretical properties. Studies of instantons for  $SU(2)$  gauge theories were performed in ref. [44]. A 48 term approximation to the fixed point action was used to verify the theoretical properties. The geometric charge was measured after one inverse blocking and it was shown that for  $Q = 1$  the instanton action was to within a few percent from the continuum action (slightly above it due to finite size effects), whereas for  $Q=0$  the action was always lower. Subsequently a simplified eight parameter form was used on which the instanton action was somewhat poorly reproduced, but such that the  $Q = 1$  boundary stayed above the entropic bound for the action.

A value of  $\chi_t = (235(10) \text{ MeV})^4$  was quoted on a  $8^4$  lattice with physical volumes of up to 1.6 fm, taking full advantage of the fact that fixed point actions can be simulated at rather large lattice spacings. However,  $\langle Q^2 \rangle$  measured on the coarse lattice was up to a factor 4 larger than on the fine lattice (for the two dimensional study much closer agreement was seen [43]). Further inverse blocking to check stability of the charge measurement was not performed.

The same eight parameter action was used in ref. [46], but they did their simulations on the fine lattice and performed an operation called smoothing: first blocking and then inverse blocking. They changed the proportionality factor  $\kappa$  in the blocking kernel, requiring that the saddle point condition is satisfied for the blocked lattice. Due to the change of  $\kappa$  the properties of the fixed point action that inspired these authors can unfortunately no longer be called upon as a justification. This smoothing satisfies the properties of cooling (the action always decreases and stays fixed for a solution) and should probably be judged as such. (See for further comments be-

low.) They consider their study exploratory and concentrate on finite temperature near and beyond the deconfinement transition.

In ref. [47] the number of terms to parametrise the fixed point action was extended to four powers of resp. the plaquette, a six-link and an eight-link Wilson loop. The latter was required to improve on the properties for the classical solutions. They achieved  $\hat{\rho}_c = 0.94$ , still considerably smaller than for  $S_{5Li}$ , and reproduced the continuum instanton action to a few percent for  $\rho > \rho_c$ . To increase the quality of the fit a constant was added, which should vanish in the continuum limit (as it drops out of the saddle point equation). Possible ramifications of this at finite coupling are not yet sufficiently understood.

After one inverse blocking insufficient smoothing is achieved to extract the pseudoparticle positions and sizes and further inverse blocking was considered computationally too expensive. Like in ref. [46], they also introduced a smoothing cycle, but now by blocking the fine lattice back to the coarse one. Such a cycle would *not* change the action when the blocking is indeed to the *same* coarse lattice. However, there are  $2^4$  different coarse sublattices associated to a fine one and in ref. [47] the smoothing cycle involved blocking to the coarse lattice shifted along the diagonal over one lattice spacing on the fine lattice. Unlike in ref. [46], the smoothing cycle will be repeated.

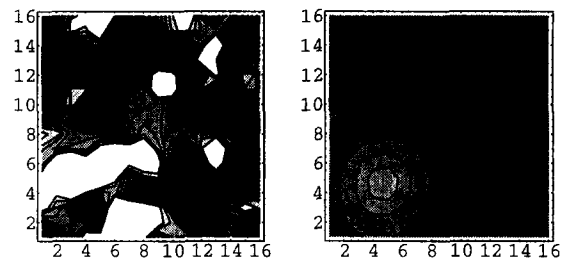


Figure 4. Example of the smoothing after 1 and 9 cycles, shown on the fine lattice. From ref. [47].

Although the fixed point nature of the action guarantees it is close to a perfect classical action it needs to be demonstrated that it preserves the topological charge at sufficiently large scales. For cooling this is argued from the local nature of the updates, not affecting the long distance behaviour. Improved cooling is in this sense less

local than ordinary cooling, and it might seem that due to the rather compact Wilson loops involved in the parametrisation of the fixed point action, the situation for the smoothing cycle is intermediate. Nevertheless, it should be pointed out that the global minimisation involved in inverse blocking, at least naively, has its effect felt over the entire lattice.

As evidence in favour of preserving long range physics, it was shown [47] that the string tension is conserved under this smoothing (unlike for the method of ref. [46], that reports changes up to 25%). That smoothing is successful in removing noise is seen in fig. 4. Somewhat surprisingly close I-A pairs remained stable for distances as close as 80% of the sum of their radii. Virtually no change is seen for up to 9 smoothing cycles. As I-A pairs are not solutions one would have expected some change. Possibly this is due to critical slowing down as can also occur for cooling [14]. It depends quite intricately on the details of the mapping implied by the smoothing cycle.

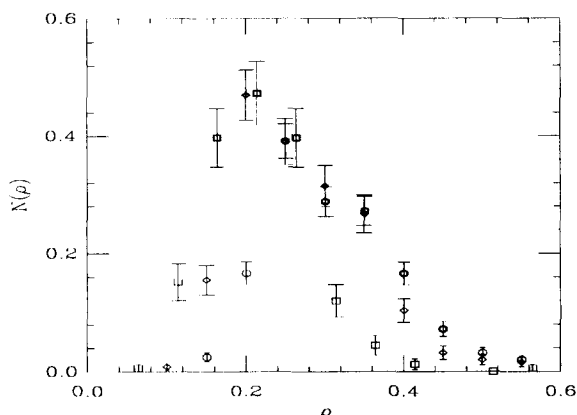


Figure 5. The  $SU(2)$  integrated instanton size distribution (integrated over bins of size 0.05 fm) for  $\beta = 1.4$  (octagons), 1.5 (diamonds) and 1.6 (squares) on a  $8^4$  lattice, with resp.  $a = 0.188$ , 0.144 and  $a = 0.116$  fm. From ref. [47].

In fig. 5 the resulting instanton size distribution is given and we refer to ref. [47] for the details on the analysis. The instanton density is approximately  $2.0 \text{ fm}^{-4}$  and the size peaks at 0.2 fm. This points to a rather dilute situation, although a study of correlations among the instantons seems to point to clustering. The sus-

ceptibility  $\chi_t = (230(10) \text{ MeV})^4$  agrees with the earlier value [44]. Cutting out instantons below 0.27 fm (see fig. 3) would give  $\chi_t = (190 \text{ MeV})^4$ , but a cut at half this value would cause no significant change. It would imply large scaling violations for the improved cooling method, which were not observed in ref. [40]. Both the susceptibility and the average size therefore disagree significantly with improved cooling.

### 3.4. Spectral flow

One can extract the topological charge by counting the number of chiral zero modes of the Dirac operator, using the Atiyah-Singer index theorem [24]. Although only valid for smooth configurations, a lattice version could in principle be defined [48],  $Q = m\kappa_P \text{Tr}(\gamma_5/(\not{D}+m))/N_f$ , with  $\kappa_P$  a renormalisation constant that depends on the lattice definition of the Dirac operator  $\not{D}$  and  $\gamma_5$  used. Due to the discretisation of the lattice no exact zero modes exist. For Wilson fermions these would-be zero modes will typically be real and give rise to poles in the euclidean path integral that are related to the “exceptional configurations”. Given the relation to instantons care is required in handling these configurations and in a recent series of papers a “pole shifting” algorithm has been proposed to remedy this problem [49]. One might also be tempted to extract the index by counting the real eigenvalues [50].

Inspired by the overlap formulation for chiral fermions [51] a much simpler method to extract the zero modes has been recently used [52]. The Wilson Dirac operator has the property that  $H(U) \equiv \gamma_5(\not{D}(U) - W(U) + 4 - m)$  is hermitian. In the continuum this operator has a spectral flow as a function of  $m$ . Non-zero modes cross zero in pairs of opposite chirality (one going up, the other going down). A zero mode is generically responsible for an isolated crossing (the direction of crossing determines the chirality). It is these properties that are expected to be robust under discretisation [51]. All that should change on the lattice is that the zero modes no longer cross at  $m = 0$  (we know that  $m$  needs to be tuned to  $m_c \neq 0$  at finite  $\beta$ , but for individual configurations the crossings will occur at different values of  $m$ ). The topological charge is now simply defined

as the number of net crossings.

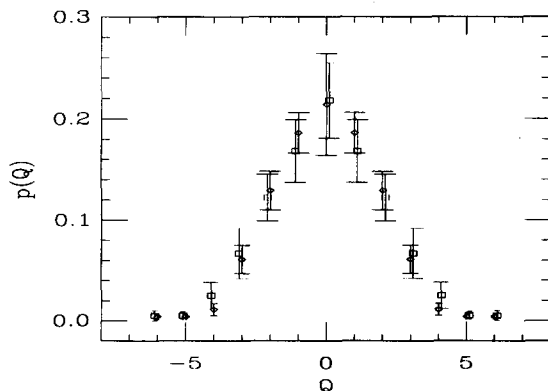


Figure 6. Comparison of the  $SU(2)$  topological charge distribution from improved cooling (squares) and from the spectral flow (diamonds), on a  $12^4$  lattice at  $\beta = 2.4$ . From ref. [52].

For very smooth instanton fields (instantons of large size), one should have near continuum behaviour and the crossing of the zero mode should occur at small values of  $m$ . Perhaps the crossing value can thus be used to define the size of the instanton [52]. One way to study the correlation between size and crossing would be to use cooling to manipulate the size of an instanton. Essential is that the spectral flow analysis is done on a coarse lattice. No smoothing is necessary. Further studies will be required, but the prospects are quite promising.

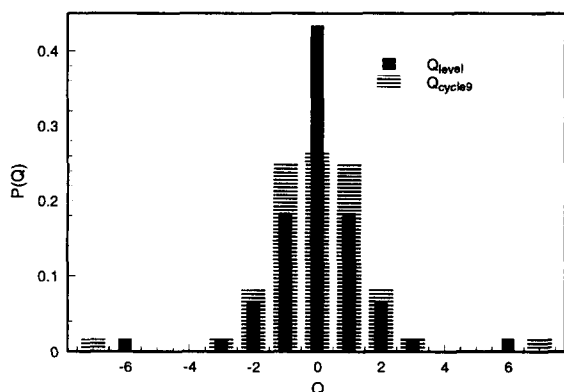


Figure 7. Comparison [52] for the fixed point action of the topological charge distribution using the spectral flow ( $Q_{\text{level}}$ ) and after nine smoothing cycles ( $Q_{\text{cycle9}}$ ) on the same configurations.

In fig. 6 a comparison is given for the topolog-

ical charge distribution generated with the Wilson action on the same lattice, measured with improved cooling [40] and with the spectral flow [52]. The agreement is excellent. From the spectral charge one extracts  $\chi_t = (184(6) \text{ MeV})^4$ .

Fig. 7 is based on 30 configurations generated with the fixed point action of ref. [47], on a  $12^4$  lattice. The charge measured after nine smoothing cycles is compared with the spectral charge on the initial rough configuration [52]. Cycling is seen to suppress the small charges. One configuration was used to trace the cause for this discrepancy [52] and it comes as an unpleasant surprise that the spectral charge was 1 without, 3 after 9 and 2 after 12 smoothing cycles.

#### 4. EPILOGUE

I report - you conclude. Who thought so much can be said about nothing. I humbly apologise to those that had hoped to find something else. I would have liked to discuss more on finite temperature and implications for the instanton liquid, on non-perturbative results in supersymmetric gauge theories as a testing ground for QCD and much more. But instantons are here to stay.

#### Acknowledgements

I thank the organisers for a job *very well* done and for entrusting me with the entertainment of the last talk. There are too many I should thank for discussions and help. Let me make an exception for Margarita García Pérez, Adriano Di Giacomo, Jeff Greensite, Ferenc Niedermayer, Misha Shifman, Edward Shuryak, Mike Teper and in particular Tom DeGrand and Anna Hasenfratz.

#### REFERENCES

1. N. Seiberg and E. Witten, Nucl.Phys. B426 (1994)19, (E) B430(1994) 485.
2. G.'t Hooft, in *High Energy Physics*, EPS conf, 1975,ed.A.Zichichi; Nucl.Phys.B 138(1978)1; S. Mandelstam, Phys.Rep. 23(1976)245.
3. G. 't Hooft, Nucl.Phys. B190[FS3](1981)455.
4. T. Suzuki and I. Yotsuyanagi, Phys.Rev. D42(1990)4257; M. Polikarpov, Nucl.Phys. B(Proc.Suppl.)53(1997)134, and ref. therein.

5. R.W. Haymaker, in *Selected Topics in Non-perturbative QCD*, eds. A. Di Giacomo and D. Diakonov, IOS Press, 1996; and ref. therein.
6. L. Del Debbio, A. Di Giacomo, G. Paffuti and P. Pieri, Phys.Lett. B355(1995)255; A. Di Giacomo, at this conference, hep-lat/9709005.
7. L. Del Debbio, M. Faber, J. Greensite and Š. Olejník, hep-lat/9708023/9709032; T.G. Kovács and E.T. Tomboulis, hep-lat/9709042.
8. S. Kato, talk at this conf., hep-lat/9709092.
9. T. Schäfer and E. Shuryak, *Instantons in QCD*, Rev.Mod.Phys(1997), hep-ph/9610451
10. P. van Baal, in *Non-perturbative approaches to QCD*, ed. D. Diakonov, hep-th/9511119.
11. B. van den Heuvel, Nucl.Phys. B488(1997)282.
12. J. Koller and P. van Baal, Nucl.Phys. B302(1988)1; P. van Baal, *ibid* B351(1991)183.
13. M. Lüscher, Nucl.Phys. B219(1983)233.
14. M. García Pérez and P. van Baal, Nucl.Phys. B429(1994)451.
15. J. Hoek, Nucl.Phys. B332(1990)530.
16. C. Taubes, Comm.Math.Phys. 86(1982)257.
17. A. Hart and M. Teper, Phys.Lett. B372(1996)261; V. Bornyakov and G. Schierholz, Phys.Lett. B384(1996)190; M. Chernodub, F. Gubarev and M. Polikarpov, hep-lat/9709039.
18. P. van Baal and N.D. Hari Dass, Nucl.Phys. B385(1992)185.
19. G. 't Hooft, Nucl.Phys. B153(1979)141; Acta Phys.Austriaca, Suppl. 22, 531 (1980).
20. G. Dali and M. Shifman, Phys.Lett. B396(1997)64; E. Witten, hep-th/9706109.
21. M. Shifman, *Nonperturbative Dynamics in Supersymmetric Gauge Theories*, extended lecture notes, hep-th/9704114.
22. I. Halperin and A. Zhitnitsky, hep-ph/9707286
23. G. 't Hooft, Phys.Rev.Lett. 37(1976)8; Phys.Rev.D14(1976)3432; Phys.Rept.142(1986)357
24. M.F. Atiyah and I.M. Singer, Ann.Math. 93(1971)119.
25. M. Fukushima, at this conf., hep-lat/9709133.
26. E. Witten, Nucl.Phys. B156(1979)269.
27. G. Veneziano, Nucl.Phys. B159(1979)213.
28. J. Smit and J. Vink, Nucl.Phys. B284(1987)234; B298(1988)557.
29. R. Alkofer, M.A. Nowak, J.J.M. Verbaarschot, and I. Zahed, Phys.Lett. B233(1989)205.
30. P. Di Vecchia, K. Fabricius, G.C. Rossi and G. Veneziano, Nucl.Phys. B192(1981)392.
31. B. Alles, M. D'Elia and A. Di Giacomo, Nucl. Phys. B494(1997)281; hep-lat/9706016 and B. Alles, talk at this conf., hep-lat/9709074.
32. B. Berg, Phys.Lett. B104(1981)475; M. Teper, Phys.Lett. B162(1985)357, B171(1986)81,86.
33. P.J. Braam and P. van Baal, Comm.Math. Phys. 122(1989)267.
34. J. Snippe, Phys.Lett. B335(1994)395.
35. M. García Pérez, A. González-Arroyo, J. Snippe and P. van Baal, Nucl.Phys. B413(1994)535
36. M. Lüscher, Nucl.Phys. B200(1982)61; D.J.R. Pugh and M. Teper, Phys.Lett. B224(1989)159
37. C. Michael and P.S. Spencer, Phys.Rev. D52(1995)4691.
38. R.C. Brower, T.L. Ivanenko, J.W. Negele and K.N. Orginos, Nucl.Phys. B(Proc.Suppl.)53(1997)547.
39. D. Smith, talk at this conf., hep-lat/9709128.
40. Ph. de Forcrand, M. García Pérez, I.-O. Stamatescu, Nucl.Phys. B(Proc.Suppl)47(1996)777, B(Proc.Suppl)53(1997)557, B499(1997)409.
41. P. Hasenfratz and F. Niedermayer, Nucl.Phys. B414(1994)785.
42. M. Lüscher, Comm.Math.Phys. 85(1982)29; A. Phillips and D. Stone, *ibid* 103(1986) 599.
43. M. Blatter, R. Burkhalter, P. Hasenfratz and F. Niedermayer, Phys.Rev. D53(1996)923; R. Burkhalter, Phys.Rev. D54(1996)4121.
44. T. DeGrand, A. Hasenfratz and D. Zhu, Nucl.Phys. B475(1996)321; B478(1996)349.
45. F. Niedermayer, Nucl.Phys. B(Proc.Suppl)53(1997)56; P. Hasenfratz, hep-lat/9709110.
46. M. Feurstein, E.-M. Ilgenfritz, M. Müller-Preussker and S. Thurner, hep-th/9611024.
47. T. DeGrand, A. Hasenfratz and T.G. Kovács, hep-lat/9705009/9709095, talk at this conf.
48. J. Smit and J. Vink, Nucl.Phys. B286(1987)285; J. Vink, Nucl.Phys. B307(1988)549.
49. W. Bardeen, A. Duncan, E. Eichten and H. Thacker, hep-lat/9705002/9705008; this conf.
50. C.R. Gatttringer, I. Hip and C.B. Lang, hep-lat/9707011/9709026, talk at this conference.
51. R. Narayanan and H. Neuberger, Nucl.Phys. B412('94)574; B443('95)305; PRL 71('93)3241
52. R. Narayanan and P. Vranas, Nucl.Phys. B(1997), hep-lat/9702005; R. Narayanan and R.L. Singleton Jr., hep-lat/9709014, this conf.